Table VI leads to the following conclusions. (i) Short treatment of PAP with dithionite removed preferentially site A iron, which is high-spin ferric in both stable states of the enzyme. Addition of ^{57}Fe(II) restored activity, but ^{57}Fe entered both A and B sites in a 53% to 47% ratio. Somewhat larger enrichment, 42% to 58%, was observed when a totally enriched ^{57}Fe sample was treated with dithionite and then reconstituted with ^{56}Fe(II).[67] In both cases, therefore, the added Fe(II) entered the A as well as the B sites, the former necessarily with a change in oxidation state; in other words, both sites had to be at least transiently unoccupied. Naively, one might have expected the short dithionite treatment to remove the A-site iron only, leaving the B-site iron intact. It appears, however, that the occupation of the two binding sites is in a dynamic equilibrium with so far unknown parameters. We do know that the "one-iron" enzyme is only slowly activated, and especially is this so in the presence of 2-mercaptoethanol.[15] It seems clear, therefore, that ligand exchange of the incoming Fe(II) [with enzyme-bound Fe(II)] occurs on a time scale fast compared to that of the oxidation leading to the active enzyme. It would be consistent with the data if the center indeed contained a μ-hydroxo bridge, since the μ-hydroxo form [Fe(II)–OH–Fe(II)] would be a likely species to be oxidized in the activation of the enzyme.

The only samples to show uncoupled high-spin Fe(II) with the parameters of the B site were the Zn- and Hg-substituted proteins; this Fe(II) species accounted for roughly 10% of the total ^{57}Fe present, and the data gave no indication whether the corresponding A site was empty or occupied by a diamagnetic ion. The majority of the ^{57}Fe in these samples occupied the A site or both the A and B sites. We note also that all Mössbauer and EPR samples that had been activated and purified by standard procedures[15] contained at most a few percent of unpaired iron of the "$g \sim 4.3$" type and no measurable Fe(II), although the number of irons per enzyme varied between 1.3 and 2 among different preparations. This observation means that there is an efficient exchange of metal ions that allows the protein to form the more stable binuclear clusters at the expense of less stable complexes with a single metal; the preparation-dependent fraction with no iron at all is presumably denatured, or the combination of apoprotein and protein with the binuclear cluster must be more stable than the single-metal complexes.

(67) Larger differential enrichment (67–33%) was recently reported for PAP from beef spleen (Cichutek, K.; Witzel, H.; Parak, F. *Hyperfine Interact.* **1988**, *42*, 885–888), but comparison with our results is difficult since neither the conditions nor the uncertainties are clearly specified.

Acknowledgment. This work was supported in part by Grant GM 16406 and in part by grants from the Australian Research Grants Committee and the University of Queensland.

Registry No. PAP, 9001-77-8; Fe, 7439-89-6.

Magnesium Ion Catalyzed P–N Bond Hydrolysis in Imidazolide-Activated Nucleotides. Relevance to Template-Directed Synthesis of Polynucleotides

Anastassia Kanavarioti,* Claude F. Bernasconi,* Donald L. Doodokyan,[1] and Diann J. Alberas

Contribution from the Chemistry Department, University of California, Santa Cruz, California 95064. *Received February 27, 1989*

Abstract: Magnesium, an ion necessary in enzymatic as well as in nonenzymatic template-directed polynucleotide-synthesizing reactions, has been found to catalyze the hydroxide ion attack on the P–N bond of selected 5′-monophosphate imidazolide derivatives of nucleotides, such as guanosine 5′-monophosphate 2-methylimidazolide (2-MeImpG), guanosine 5′-monophosphate imidazolide (ImpG), and adenosine 5′-monophosphate 2-methylimidazolide (2-MeImpA). Calcium ion behaves similarly, but quantitatively the effects are smaller. Pseudo-first-order rate constants of 2-MeImpG and ImpG hydrolysis as a function of Mg^{2+} concentration have been obtained in the range $6 \leq pH \leq 10$ at 37 °C. Mg^{2+} catalysis is particularly effective around pH 10 where a 0.02 M concentration leads to 15-fold acceleration and a 0.2 M concentration to a 115-fold acceleration of the rate. At other pH values Mg^{2+} catalysis is less dramatic, mainly because the noncatalyzed reaction is faster. Mg^{2+} catalysis is attributed to the reaction of the zwitterionic form of the substrate ($SH^{\pm}$, imidazolide moiety protonated) with OH^- rather than reaction of the anionic form (S^-, imidazolide moiety deprotonated) with water. This conclusion is based on a study of the N-methylated substrates *N*-MeImpG and 1,2-diMeImpG, respectively, which were generated in situ by the equilibrium reaction of ImpG with *N*-methylimidazole and 2-MeImpG with 1,2-dimethylimidazole, respectively. In contrast, in the *absence* of Mg^{2+} the reaction of S^- with water competes with the reaction of $SH^{\pm}$ with OH^-. The present study bears on the mechanism of the Mg^{2+}-catalyzed template-directed synthesis of oligo- and polynucleotides derived from 2-MeImpG and on the competition between oligonucleotide synthesis and hydrolysis of 2-MeImpG.

Reactions of imidazolide-activated nucleotides or nucleotide analogs are of interest because these activated monomers have been used successfully in modeling the nonenzymatic, template-directed synthesis of oligonucleotides.[2-4] In these syntheses a poly- or oligonucleotide, acting as the template, directs the polymerization of the complementary mononucleotide on the basis of Watson–Crick base-pairing interactions in a similar fashion as DNA/RNA directs the synthesis of a daughter polynucleotide using triphosphate nucleotides as the activated monomers.[5]

(1) D.L.D. was supported by NASA Grant No. NCC2-166 to the late Prof. D. H. White of the University of Santa Clara.
(2) Kanavarioti, A.; White, D. H. *Origins Life* **1987**, *17*, 333.
(3) Inoue, T.; Orgel, L. E. *Science* **1983**, *219*, 859.
(4) Orgel, L. E. *J. Theor. Biol.* **1986**, *123*, 127.

(5) A complete replication cycle consists of the formation of a daughter strand that is complementary to the template, followed by the use of the daughter strand as template to form its complementary strand, the parent molecule.

0002-7863/89/1511-7247$01.50/0

Scheme I

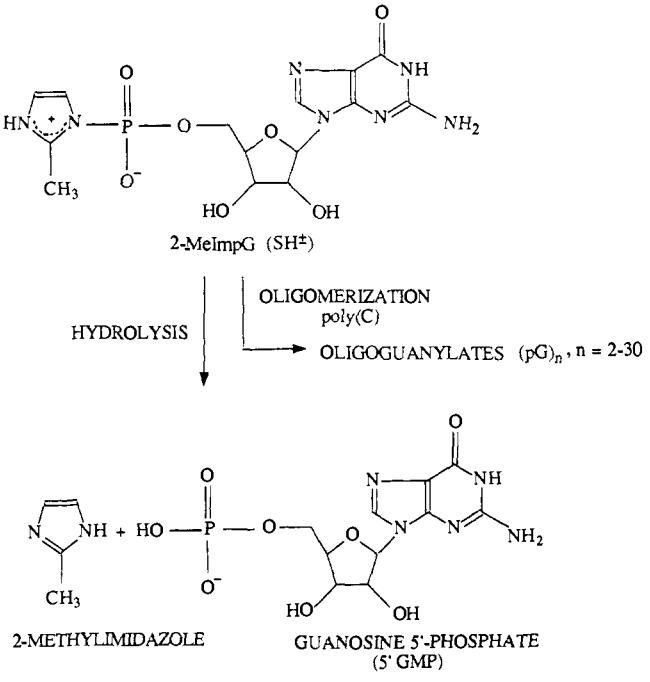

Template-directed reactions are thought to have played an important role in chemical evolution before the advent of efficient enzymatic systems.[4]

Among the most efficient template-directed oligomerization reactions known is the reaction of guanosine 5′-monophosphate 2-methylimidazolide (2-MeImpG) on polycytidylate, poly(C) (Scheme I). An extensive study[6] of this reaction has shown that oligomerization leads to oligoguanylates, $(pG)_n$ where $n = 2–30$, with approximately 90% efficiency. Conditions for optimal efficiency are pH 8 and 0.2 M Mg^{2+} concentration. The oligomerization reaction, though, is in competition with the hydrolysis reaction that forms guanosine 5′-monophosphate (5′-GMP), an unreactive monomer. Thus, it is critical to determine the rates of 2-MeImpG hydrolysis in the presence of magnesium in order to establish the conditions under which hydrolysis is in competition with the oligomerization. A preliminary study[7] of the hydrolysis of 2-MeImpG indicated that hydrolysis is much slower than template-directed elongation, but the potentially important effect of Mg^{2+} was not investigated. Another motivation for studying the hydrolysis is that the polymerization reaction has a similar chemistry as the hydrolysis and hence such a study should be able to teach us something about the mechanism of the template-directed reaction.

We now report a detailed investigation of the hydrolysis of 2-MeImpG in the presence of 0–0.50 M Mg^{2+} in the range $6 \leq pH \leq 12.4$ at 37 °C and a more limited study of the hydrolysis of guanosine 5′-monophosphate imidazolide (ImpG). The results show that catalysis by Mg^{2+} becomes increasingly important with increasing pH in a pH region where the imidazole moiety loses its proton, thereby becoming a poor leaving group. Selected experiments with 1,2-diMeImpG and *N*-MeImpG (the N-methylated derivatives of 2-MeImpG and ImpG, respectively) were performed, in order to distinguish between kinetically equivalent mechanisms by which magnesium is catalyzing the hydrolysis. These N-methylated derivatives were formed in situ from 2-MeImpG and ImpG, respectively, in the presence of 1,2-dimethylimidazole (1,2-diMeIm) and *N*-methylimidazole (N-MeIm), respectively. A few experiments were performed with calcium ion, and one experiment was carried out with the adenosine derivative (2-MeImpA), in order to evaluate a possible role played by the nucleic acid base moiety.

(6) Inoue, T.; Orgel, L. E. *J. Mol. Biol.* **1982**, *162*, 201.
(7) Kanavarioti, A. *Origins Life* **1986**, *17*, 85.

Table I. Kinetics of Hydrolysis of ImpG and 2-MeImpG as a Function of pH in the Absence of Mg^{2+} at 37 °C[a]

ImpG		2-MeImpG	
pH	$10^2 k_{obsd}$, h^{-1}	pH	$10^2 k_{obsd}$, h^{-1}
4.11	53.5	6.02	3.32
4.48	57.4	6.82	2.49
4.78	56.1	7.32	1.57
5.78	32.9	7.63	1.11
6.43	15.2	7.82	0.902
7.22	2.68	8.13	0.513
7.75	0.646	8.49	0.356
7.96	0.84	8.66	0.258
8.27	0.307	8.96	0.163
8.36	0.43	9.40	0.070
8.78	0.128	9.69	0.045
8.80	0.11	10.38	0.022
9.28	0.073	11.67	0.042
10.34	0.033	12.03	0.066
11.67	0.38	12.34	0.101
12.03	0.73	12.43	0.121
12.34	1.28	12.60	0.171
12.43	1.69	12.75	0.246
12.60	2.77		
12.75	3.34		

[a] pH measurements were performed at room temperature with a microelectrode in the actual sample. Ionic strength was kept at 1.75 M with NaCl. With ImpG, rates in the pH range 4.11–4.78 were obtained in a 0.05 M acetate buffer; at pH 5.78 and 6.43 in a 0.5 M MES buffer; at pH 7.22 in a 0.5 M Im buffer; in the pH range 7.75–8.36 in a 0.5 M HEPES buffer; and in the range 8.78–10.34 in a 0.5 M CHES buffer. With 2-MeImpG, rates at pH 6.02 were obtained in a 0.5 M MES buffer; at pH 6.82 in a 0.5 M HEPES buffer; in the pH range 7.32–8.96 in a 0.5 M 2-MeIm buffer; at pH 9.40, 9.69, and 10.38 in a 0.5 M CHES buffer. The solutions at pH ≫ 11.67 were made with NaOH, and the pH values were measured in mock solution with standard pH electrodes.

Experimental Section

Materials. The sodium salts of 2-MeImpG, 2-MeImpA, and ImpG were synthesized according to a known procedure.[8] Solvents used were HPLC quality. Buffers and other reagents including magnesium and calcium chloride were purchased from Sigma or Aldrich. They are abbreviated as follows: imidazole, Im; 2-methylimidazole, 2-MeIm; 1,2-dimethylimidazole, 1,2-diMeIm; *N*-methylimidazole, *N*-MeIm; 2-[*N*-cyclohexylamino]ethanesulfonic acid, CHES; *N*-(2-hydroxyethyl)-piperazine-*N*′-2-ethanesulfonic acid, HEPES; 2-[*N*-morpholino]ethanesulfonic acid, MES.

Kinetic Measurements. Samples were prepared in HPLC-grade water. They contained 0.001 M of the nucleotide derivative, usually 0.5 M of buffer and ionic strength of 1.75 M maintained with NaCl, unless otherwise noted. The reactions were run at 37 ± 0.2 °C. Most of the samples were prepared directly in the vials from where the analyses were carried out. The reaction solutions had a total volume of 800 or 1000 μL and were placed inside the thermostated autosampler of a 1090M Hewlett-Packard liquid chromatograph (HPLC) where the analysis was performed on 10-μL samples and recorded automatically. The initial phases of the work with 2-MeImpG were carried out at the NASA/Ames Research Center using a nonthermostated autosampler of a 1084B Hewlett-Packard HPLC, which required a more cumbersome procedure. Here samples of 40 μL prepared in 1.5 mL of polypropylene (Fisherbrand) test tubes, incubated at 37 ± 0.5 °C, were withdrawn at selected times, quenched with a slightly basic EDTA solution to chelate Mg^{2+}, and then either analyzed immediately or kept at −20 °C for 1–3 days before analysis. In this case it was found to be more accurate to express substrate decomposition as percent HPLC units of the total sample, since at the wavelength where the reaction was monitored, 254 nm, both the substrate, 2-MeImG, and the product, 5′-GMP, exhibit identical extinction coefficients.

UV absorbances were monitored at 254 nm where none of the imidazoles used absorb. The absorbance observed in this region comes from the nucleotide moiety. Pseudo-first-order kinetics were obtained for up to 4 half-lives of reaction, except in the cases where the reactions were very slow. No sample was left incubating for more than 3 weeks.

The inertness of the buffers was inferred from the absence of any unidentified peaks in the chromatograms. Even though 5′-GMP pre-

(8) Joyce, G. F.; Inoue, T.; Orgel, L. E. *J. Mol. Biol.* **1984**, *176*, 279.

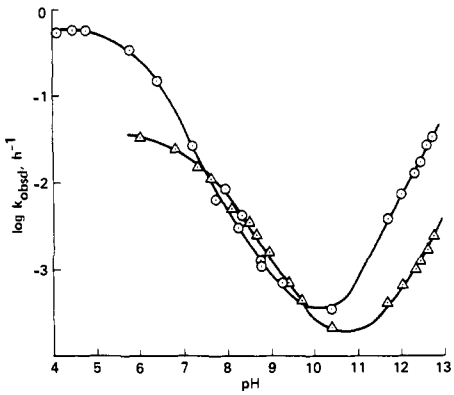

Figure 1. Rate–pH profile of the hydrolysis of ImpG (circles) and 2-MeImpG (triangles) at 37 °C.

Scheme II

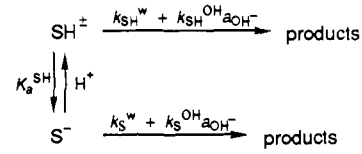

cipitates in the presence of Mg^{2+}, the small amount of 5′-GMP formed by the hydrolysis of the substrates (up to 0.001 M) did not create any cloudiness. Rate and equilibrium constants were calculated using least-squares analysis. For the determination of each rate constant 6–15 samples were used and the standard error was less than 5%, unless otherwise noted. The pH was measured at room temperature either in mock solutions excluding the substrate or directly in the test tubes using a microelectrode (MI 410 by Microelectrodes, Inc.).

HPLC Analysis. Analysis was performed on a 1084B Hewlett-Packard LC chromatograph or on a 1090M Hewlett-Packard LC chromatograph equipped with a diode array detector and a thermostated autosampler. A 25-cm reversed-phase Adsorbosphere HS C-18 column (5 or 7 μ) supplied by Alltech or a 20-cm reversed-phase ODS column (5 μ) was used. Chromatographic conditions had been developed earlier[9] and are as follows. Mobile phase: solvent A, 0.02 M potassium dihydrogen phosphate (pH 6.5); solvent B, acetonitrile–water (30:70). Gradient elution, 0–30% B in 13 min. Retention times with the 1090M HPLC on the ODS column are the following: 5′-GMP, 3.2; *N*-MeImpG, 9.8; 2-MeImpG, 10.2; 1,2-diMeImpG, 10.5; ImpG, 10.7. Retention times for 5′-AMP, 6.3, and 2-MeImpA, 12.8, were obtained with gradient elution, 0–30% B in 15 min.

Results

Hydrolysis of 2-MeImpG and ImpG in the Absence of Mg^{2+}. The hydrolysis of 2-MeImpG and ImpG was studied as a function of pH at 37 °C. The hydrolysis products of 2-MeImpG were 5′-GMP and 2-MeIm; those of ImpG were 5′-GMP and Im. Some minor byproducts, identified as guanosine and guanosine 3′,5′-cyclic monophosphate,[9] were observed at the high end of the pH range, but they never amounted to more than 0.5% of the total. The results are summarized in Table I. Figure 1 shows the rate–pH profile of the pseudo-first-order rate constant (k_{obsd}) of hydrolysis of the P–N bond in 2-MeImpG (△) and in ImpG (○).

The minimum mechanism that describes the results is illustrated in Scheme II and obeys the rate law given by eq 1, in which $SH^{\pm}$ represents the zwitterionic form, and S^- the anionic form of the substrate (2-MeImpG or ImpG). The plateau at low pH represents $k_{obsd} = k_{SH}^{w}$ ($pH \ll pK_a^{SH}$, $k_{SH}^{OH}a_{OH^-} \ll k_{SH}^{w}$; $(k_S^{w} + k_S^{OH}a_{OH^-})K_a^{SH}/a_{H^+} \ll k_{SH}^{w}$); the descending portion is approximated by $k_{obsd} \approx k_{SH}^{w}a_{H^+}/K_a^{SH}$ ($pH \gg pK_a^{SH}$, $k_{SH}^{OH}a_{OH^-} \ll k_{SH}^{w}$; $k_S^{w} + k_S^{OH}a_{OH^-} \ll k_{SH}^{w}$); the plateau at high pH corresponds to $k_{obsd} = k_{SH}^{OH}K_w/K_a^{SH} + k_S^{w}$ with $K_w = a_{H^+}a_{OH^-}$ ($k_{SH}^{OH}a_{OH^-} \gg k_{SH}^{w}$; $k_{SH}^{OH}K_w/K_a^{SH} + k_S^{w} \gg k_S^{OH}a_{OH^-}$; the ascending phase at high pH represents $k_{obsd} = k_S^{OH}a_{OH^-}$.

(9) Kanavarioti, A.; Doodokyan, D. L. *J. Chromatogr.* **1987**, *389*, 334.

Table II. Kinetics of Hydrolysis of 2-MeImpG as a Function of pH at Various Mg^{2+} Concentrations, at 37 °C[a]

0.02 M Mg^{2+}		0.1 M Mg^{2+}		0.2 M Mg^{2+}	
pH	10^2k_{obsd}, h^{-1}	pH	10^2k_{obsd}, h^{-1}	pH	10^2k_{obsd}, h^{-1}
6.01	3.54	5.98	3.70	5.93	3.63
6.81	2.65	6.78	2.79	6.74	3.28
7.60	1.76	7.26	2.43	7.27	3.10
7.79	1.36	7.57	2.17	7.58	2.80
8.42	1.00	7.77	1.95	7.76	2.85
8.61	0.783	8.11	1.55	8.09	2.50
8.91	0.581	8.42	1.57	8.43	2.58
9.33	0.308	8.60	1.41	8.61	2.56
9.61	0.318	8.91	1.46	8.91	2.51
9.76	0.330	9.25	1.59	9.17	2.75
10.02	0.321	9.65	1.39	9.61	2.42

[a] pH measurements were performed at room temperature in mock solutions. Ionic strength was kept at 1.75 M with NaCl. Rates at pH ≈ 6.0 were obtained in a 0.5 M MES buffer; at pH ≈ 6.8 and 7.3 in a 0.5 HEPES buffer; in the pH range 7.57–8.91 in a 0.5 M 2-MeIm buffer; and in the range 9.17–10.02 in a 0.25 M CHES buffer.

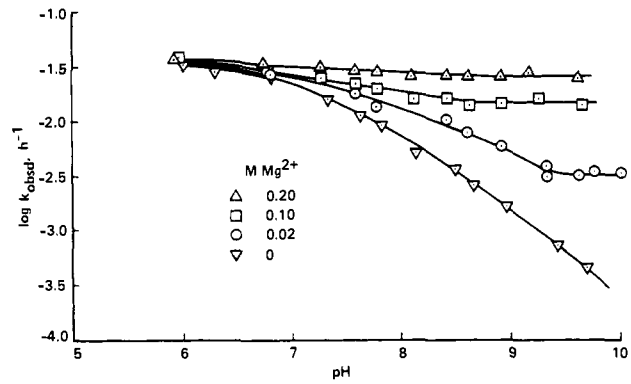

Figure 2. Rate–pH profile of the hydrolysis of 2-MeImpG at various Mg^{2+} concentrations at 37 °C.

$$k_{obsd} = \frac{k_{SH}^{w} + k_{SH}^{OH}a_{OH^-} + \frac{K_a^{SH}}{a_{H^+}}(k_S^{w} + k_S^{OH}a_{OH^-})}{1 + \frac{K_a^{SH}}{a_{H^+}}} \quad (1)$$

The above analysis shows that the reactions of $SH^{\pm}$ with OH^- and of S^- with water are kinetically indistinguishable (plateau at high pH, $k_{obsd} = k_{SH}^{OH}K_w/K_a^{SH} + k_S^{w}$). In the Discussion it will be shown that the k_{SH}^{OH} pathway is probably dominant with 2-MeImpG while k_S^{w} is dominant with ImpG. Table VIII summarizes the parameters k_{SH}^{w}, $k_{SH}^{OH}K_w/K_a^{SH} + k_S^{w}$, k_S^{OH}, and pK_a^{SH} that give the best fit with the data.

Effect of Mg^{2+} on the Hydrolysis of 2-MeImpG, ImpG, and 2-MeImpA. The hydrolysis of the P–N bond in 2-MeImpG was investigated over a range $6 < pH < 10$ in the presence of different concentrations of Mg^{2+}. Experiments at $pH > 10$ were precluded because of precipitation of magnesium hydroxide. Most kinetic results are summarized in Table II. Figure 2 shows rate–pH profiles of k_{obsd} at 0, 0.02, 0.1, and 0.2 M Mg^{2+}. Additional data in the presence of a large range of Mg^{2+} concentrations at pH 8.09, 8.69, and 9.09 are in Table S1 of the supplementary material.[10] Figure 2 shows that the presence of Mg^{2+} sharply attenuates the decrease in k_{obsd} with increasing pH. For example, at 0.2 M Mg^{2+} k_{obsd} differs by 1.5-fold between pH 6.0 and 9.6 while in the absence of Mg^{2+} this difference is 74-fold. We also note that at all Mg^{2+} concentrations k_{obsd} reaches a plateau at $pH > 9$.

Similar experiments were carried out with ImpG at pH 7.98 and 8.36 and with 2-MeImpA at pH 9.08. The results are reported in Table S2 of the supplementary material.[10] Figure 3 shows plots

(10) See paragraph concerning supplementary material at the end of this paper.

Table III. Initial Slopes of Plots of k_{obsd} vs Mg^{2+} Concentration

	slope, M^{-1} h^{-1}		
pH	2-MeImpG	2-MeImpA	ImpG
6.78	0.037		
7.29	0.077		
7.96			0.082
8.09	0.097		
8.36			0.071
8.69	0.093		
9.09	0.099	0.094	

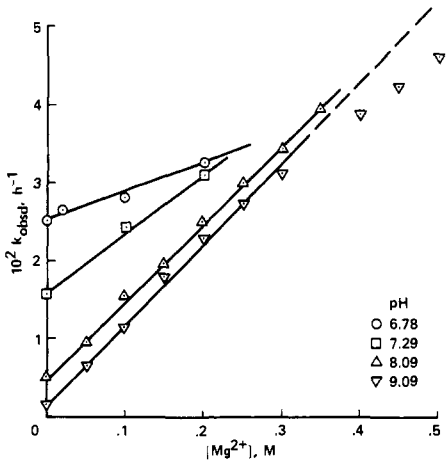

Figure 3. Hydrolysis of 2-MeImpG as a function of $[Mg^{2+}]$ at various pH's, 37 °C.

of k_{obsd} vs $[Mg^{2+}]$ for 2-MeImpG; Figure 4 shows plots for ImpG and 2-MeImpA. Some of these plots display slight downward curvature at high $[Mg^{2+}]$, which suggests formation of an association complex between the substrate and Mg^{2+}. With ImpG curvature is evident at $[Mg^{2+}] \geq 0.2$ M and appears sufficiently strong to constitute good evidence for the accumulation of such a complex. With 2-MeImpG and 2-MeImpA the curvature is rather weak and provides less compelling evidence that the complex accumulates significantly.

There are two kinetically equivalent mechanistic alternatives that may account for the effect of magnesium. In the first there is complexation of the S^- form of the substrate with the metal ion, which presumably facilitates nucleophilic attack by water and hydroxide ion. This leads to an extension of Scheme II as shown in Scheme III. K_M is the association equilibrium constant while k_{SM}^{w} and k_{SM}^{OH} are the rate constants for water and OH^- attack on the complex, respectively. Note the $k_S^{OH}a_{OH^-}$ term has been omitted from the scheme because it is negligible in the pH range investigated.

k_{obsd} is given by

$$k_{obsd} = \left\{k_{SH}^{w} + k_{SH}^{OH}a_{OH^-} + \frac{K_a^{SH}}{a_{H^+}}k_S^{w} + \frac{K_a^{SH}}{a_{H^+}}K_M[Mg^{2+}] \times (k_{SM}^{w} + k_{SM}^{OH}a_{OH^-})\right\} \Big/ \left\{1 + \frac{K_a^{SH}}{a_{H^+}}(1 + K_M[Mg^{2+}])\right\} \quad (2)$$

The (initial) slopes of the plots of k_{obsd} vs $[Mg^{2+}]$ (Figures 3 and 4), summarized in Table III, are given by eq 3 ($K_M[Mg^{2+}] \ll 1$)

$$\text{slope} = \frac{K_M}{1 + \frac{a_{H^+}}{K_a^{SH}}}(k_{SM}^{w} + k_{SM}^{OH}a_{OH^-}) \quad (3)$$

which at $pH \gg pK_a^{SH}$ simplifies to

$$\text{slope} = K_M(k_{SM}^{w} + k_{SM}^{OH}a_{OH^-}) \quad (4)$$

Figure 3 shows the predicted increase in slope arising from the change from $a_{H^+}/K_a^{SH} \sim 1$ to $a_{H^+}/K_a^{SH} \ll 1$; the $k_{SM}^{OH}a_{OH^-}$ term

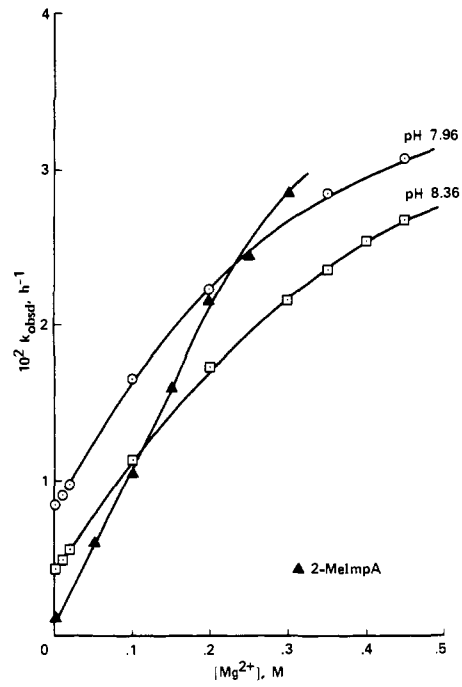

Figure 4. Hydrolysis of ImpG as a function of $[Mg^{2+}]$ at pH 7.96 and 8.36 and of 2-MeImpA at pH 9.08 at 37 °C.

Scheme III

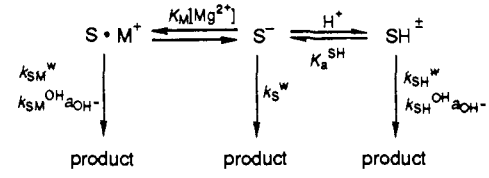

Scheme IV

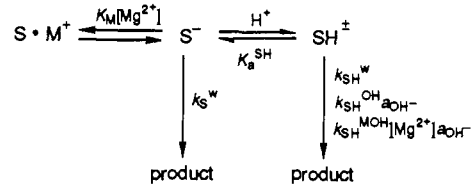

is seen to remain negligible in the pH range investigated.

Equation 2 is also able to account for the absence of a pH dependence for $pH \geq 9$ ($pH \gg pK_a^{SH}$). Under these conditions eq 2 simplifies to

$$k_{obsd} = \frac{K_M[Mg^{2+}]k_{SM}^{w}}{1 + K_M[Mg^{2+}]} \quad (5)$$

As attractive as Scheme III might be (see also Discussion), it is difficult to reconcile it with data on the hydrolysis of the N-methylated substrates presented below. These data suggest a mechanism involving metal ion catalysis of the hydrolysis of the $SH^{\pm}$ form rather than the S^- form. The most likely version of such a mechanism is shown in Scheme IV ($k_S^{OH}a_{OH^-}$ has again been omitted). k_{obsd} for Scheme IV is given by

$$k_{obsd} = \frac{k_{SH}^{w} + k_{SH}^{OH}a_{OH^-} + \frac{K_a^{SH}}{a_{H^+}}k_S^{w} + k_{SH}^{MOH}[Mg^{2+}]a_{OH^-}}{1 + \frac{K_a^{SH}}{a_{H^+}}(1 + K_M[Mg^{2+}])} \quad (6)$$

The $k_{SH}^{MOH}[Mg^{2+}]a_{OH^-}$ term may either represent OH^- attack on a complex between $SH^{\pm}$ and the metal ion or nucleophilic attack on $SH^{\pm}$ by $MgOH^+$ (see Discussion). If there is a complex

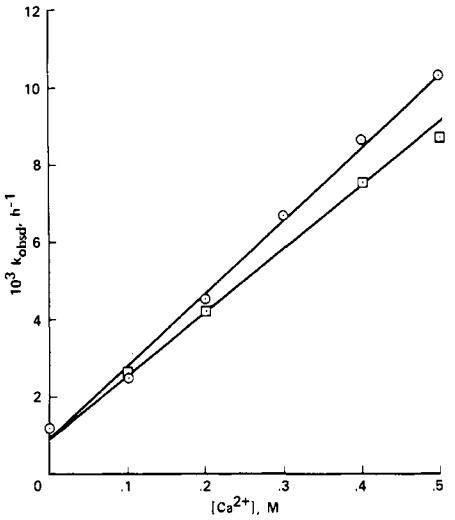

Figure 5. Hydrolysis of 2-MeImpG (circles) and ImpG (squares) as a function of Ca^{2+} concentration at pH 8.80, 37 °C.

formed between $SH^{\pm}$ and Mg^{2+}, it is likely to have a smaller complexation equilibrium constant than K_M for the complex between S^- and Mg^{2+} (see Discussion), and hence the curvature in the plots of k_{obsd} vs $[Mg^{2+}]$ is attributed to this latter complex rather than to the former, just as in Scheme III.

According to eq 6 the (initial) slopes in Figures 3 and 4 are given by

$$\text{slope} = \frac{k_{SH}^{MOH} a_{OH^-}}{1 + \frac{K_a^{SH}}{a_{H^+}}} = \frac{K_{SH}^{MOH} K_w}{K_a^{SH} + a_{H^+}} \quad (7)$$

which simplifies to

$$\text{slope} = k_{SH}^{MOH} K_w / K_a^{SH} \quad (8)$$

at pH $\gg$ pK_a^{SH}. The plateau values of k_{obsd} in Figure 2 at pH > 9 correspond to

$$k_{obsd} = \frac{k_{SH}^{MOH} K_w [Mg^{2+}]}{K_a^{SH}(1 + K_M[Mg^{2+}])} \quad (9)$$

k_{SH}^{MOH} and K_M values for 2-MeImpG, ImpG, and 2-MeImpA calculated on the basis of eq 8 and 9 are summarized in Table VIII.

Effect of Ca^{2+} on the Hydrolysis of 2-MeImpG and ImpG. In a limited number of experiments Ca^{2+} was also found to catalyze the reaction, but to a lesser extent than Mg^{2+}. Rates were obtained at pH 8.80 ± 0.04 in a 0.5 M CHES buffer with ionic strength kept constant at 1.75 M with NaCl. Table S3 of the supplementary material[10] includes the data for both substrates. Plots of k_{obsd} vs $[Ca^{2+}]$ are linear (Figure 5) and exhibit slopes 1.89 × 10^{-2} M^{-1} h^{-1} (2-MeImpG) and 1.56 × 10^{-2} M^{-1} h^{-1} (ImpG), respectively.

Hydrolysis of 1,2-diMeImpG and *N*-MeImpG. The experiments described in this section were aimed at distinguishing between Schemes III and IV as interpretations of Mg^{2+} catalysis. They do not constitute a complete kinetic study of these reactions but nevertheless provide good approximations of some kinetic parameters. *N*-MeImpG and 1,2-diMeImpG were formed in situ by the equilibrium reactions shown in eq 10 and 11. In most of

$$\text{2-MeImpG } (SH^{\pm}) + \text{1,2-diMeIm} \overset{K_N}{\rightleftharpoons} \text{1,2-diMeImpG } (SMe^{\pm}) + \text{2-MeIm} \quad (10)$$

$$\text{ImpG } (SH^{\pm}) + \textit{N}\text{-MeIm} \overset{K_N}{\rightleftharpoons} \textit{N}\text{-MeImpG } (SMe^{\pm}) + \text{Im} \quad (11)$$

the experiments 2-MeIm (eq 10) or Im (eq 11) were added to the reaction mixture at concentrations much higher than those of total 2-MeImpG (or ImpG). This procedure assured that the equilibrium position of eq 10 and 11 would not be altered during a kinetic run; i.e., the ratios [1,2-diMeImpG]/[2-MeImpG] (or [N-MeImpG]/[ImpG]) would stay constant and be given by eq 12 and 13, respectively.

$$\frac{[\text{1,2-diMeImpG}]}{[\text{2-MeImpG}]} = K_N \frac{[\text{1,2-diMeIm}]_0}{[\text{2-MeIm}]_0} = K_N' \quad (12)$$

$$\frac{\textit{N}\text{-MeImpG}}{[\text{ImpG}]} = K_N \frac{[\textit{N}\text{-MeIm}]_0}{[\text{Im}]_0} = K_N' \quad (13)$$

Table IV. Kinetics of Hydrolysis of 2-MeImpG in the Presence of 1,2-diMeIm and 2-MeIm at 37 °C

pH	[1,2-diMeIm],[a] M	[2-MeIm],[a] M	K_N'[b]	$[Mg^{2+}]$, M	$10^2 k_{obsd}$, h^{-1}
8.20	0.205	0.005	2.92	0	6.4
				0.02	8.9
				0.05	13
				0.10	17
				0.40	45.2
				0.50	42.5
8.75	0.35	0.0078	3.55	0	4.4
				0.01	6.5
				0.02	8.7
				0.04	12.6
				0.05	14.2
				0.08	19.8
				0.10	21.5
				0.20	29.2
				0.35	39.6
				0.45	41.4
8.48	0.568	0.0334	1.34	0	4.2
				0.25	22.5
				0.50	29.3
	0.284	0.0167	1.34	0	3.7
				0.25	22.7
				0.50	31.5
8.48	0.085	0.0020	3.32	0	6.02
	0.071	0.0017			5.16
	0.057	0.0013			5.14
	0.043	0.0010			5.14
	0.028	0.0007			5.32
	0.17	0.0020	6.64	0	6.98
	0.142	0.0017			6.87
	0.114	0.0013			6.91
	0.085	0.0010			6.97
	0.057	0.0007			6.92
8.50	0.87	0.100	0.687	0	2.55
	0.696	0.08			2.40
	0.058	0.067			2.28
	0	0.08			0.20

[a] Concentrations refer to free base calculated from pH measurements, total buffer concentration, and the pK_a's as measured at room temperature; pK_a = 8.18 (2-MeIm), 8.37 (1,2-diMeIm). [b] K_N' defined in eq 12; K_N = 0.079 determined by HPLC.

The evidence for the formation of the two *N*-methylated derivatives is as follows: solutions of ImpG (2-MeImpG) in the presence of added *N*-MeIm (1,2-diMeIm) result in the formation of a new compound identified by HPLC to have a UV–vis spectrum almost indistinguishable from the one of the parent compound. On HPLC the corresponding *N*-methyl derivative elutes very close to the parent compound (see the Experimental Section), suggesting structural similarity between the two compounds. It was also confirmed that the product of hydrolysis of the new compounds was 5′-GMP, just as for the parent compound, indicating that the former are indeed phosphorylimidazolide-activated guanylic acids. In most of the solutions one could simultaneously observe all three guanosine derivatives, for example, ImpG, *N*-MeImpG, and pG.

In order to evaluate rate constants we monitored disappearance of ImpG or *N*-MeImpG depending on which one was present at higher equilibrium concentration. In the situations where ImpG or *N*-MeImpG were both present at similar concentrations, each could be observed to disappear with the same rate constant,

Table V. Hydrolysis of 2-MeImpG in the Presence of 1,2-diMeIm and 2-MeIm in NaOH Solutions, without Mg^{2+} at 37 °C

[NaOH], M	$10^3 k_{obsd}$, h^{-1}				
	$K_N' = 0$[a,b]	$K_N' = 15.8$[a,c]	Δ	$K_N' = 19.75$[a,d]	Δ
0.005	≈0.03[e]	2.92	≈2.62		
0.01	0.422	1.73	1.31	1.69	1.27
0.02	0.66	1.025	0.365	1.14	0.48
0.04	1.01	1.43	0.44	1.28	0.27
0.05	1.21	1.60	0.39	1.66	0.45
0.08	1.71				

[a] K_N' defined in eq 12; K_N = 0.079 determined by HPLC; [2-MeImpG] = 5×10^{-4} M. [b] No 1,2-diMeIm/2-MeIm added; data from Table I. [c] [1,2-diMeIm] = 0.5 M, [2-MeIm] = 0.0025 M. [d] [1,2-diMeIm] = 0.5 M, [2-MeIm] = 0.002 M. [e] Extrapolated from Figure 1.

Scheme V

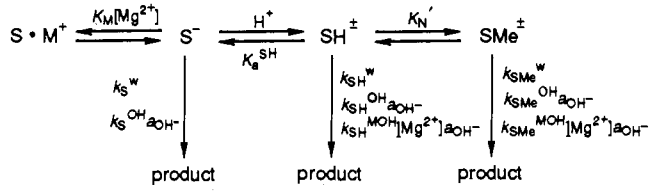

showing that the two compounds were present in a rapid equilibrium. The disappearance of 2-MeImpG/1,2-diMeImpG was monitored in a similar way.

Another way to show the presence of this rapid equilibrium was to first incubate a concentrated solution of ImpG and *N*-MeIm at 37 °C at neutral pH for a few minutes to form an excess of *N*-MeImpG. When this solution was diluted to the conditions of a typical kinetic experiment, the same kinetic behavior was observed as for solutions that had been prepared by a more standard procedure. It should be noted, though, that, at very high pH or at high Mg^{2+} concentrations, the rapid equilibrium conditions start to break down; i.e., the formation of $SMe^{\pm}$ becomes partially rate-limiting.

We now describe the kinetic results in detail.

1,2-diMeImpG. The kinetic data are summarized in Tables IV (pH 8.20–8.75) and V ([NaOH] = 0.005–0.08 M). We first discuss the results at pH 8.20–8.75. They show that in the presence of 1,2-diMeIm the rate of hydrolysis of 2-MeImpG increases strongly and that this increase is substantially augmented by the presence of magnesium ion. For example, at pH 8.48 hydrolysis occurs with $k_{obsd} = 3.56 \times 10^{-3}$ h^{-1} (Table I), whereas in the presence of 0.568 M 1,2-diMeIm/0.0334 M 2-MeIm, $k_{obsd} = 4.2 \times 10^{-2}$ h^{-1}, an approximately 12-fold increase. Addition of 0.5 M Mg^{2+} results in a further 7-fold acceleration (k_{obsd} = 0.293 h^{-1}).

These rate increases can be accounted for by assuming that 1,2-diMeImpG, which is a zwitterionic compound ($SMe^{\pm}$) just as $SH^{\pm}$, undergoes the same reactions as $SH^{\pm}$ and is of comparable reactivity, and much more reactive than S^-. This is shown in the extended Scheme V (K_N' defined in eq 12; the scheme includes the $k_S^{OH}a_{OH^-}$ pathway since experiments were also performed at high pH).

We start by providing a qualitative understanding of how Scheme V behaves kinetically. For this purpose we shall assume that $SMe^{\pm}$ and $SH^{\pm}$ have the same reactivity; i.e., $k_{SMe}^{w} = k_{SH}^{w}$, $k_{SMe}^{OH} = k_{SH}^{OH}$, and $k_{SMe}^{MOH} = k_{SH}^{MOH}$. At pH $\ll pK_a^{SH}$, $[S^-]$ and $[S{\cdot}M^+]$ are negligible, and the rates will be unaffected by the presence or absence of 1,2-diMeIm. This is because all the material is either in the $SH^{\pm}$ or $SMe^{\pm}$ form, which are equally reactive, and hence a shift from $SH^{\pm}$ to $SMe^{\pm}$ is of no kinetic consequence. On the other hand, at pH >(≫) pK_a^{SH} the dominant form is S^-. In this situation a shift toward the highly reactive $SMe^{\pm}$ will be mainly at the expense of the weakly reactive S^-, with a corresponding increase in the rate.

The data summarized in Table IV were all obtained at pH >(≫) pK_a^{SH} where, on the basis of the above considerations, rate accelerations are expected. A quantitative analysis of these data can be based on eq 14 in the absence of Mg^{2+} and on eq 15 in the presence of Mg^{2+}. K_N was directly determined from the ratio

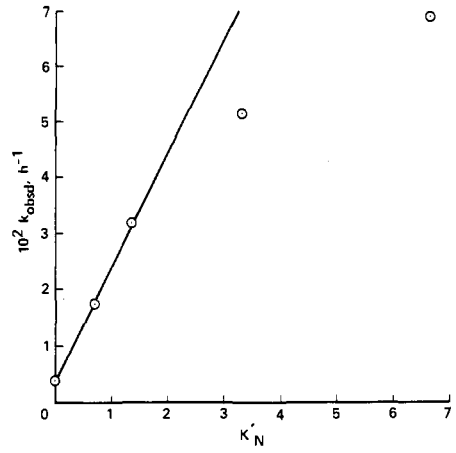

Figure 6. Hydrolysis of 2-MeImpG in the presence of 1,2-diMeIm and 2-MeIm. k_{obsd} shown as a function of K_N' (K_N' defined in eq 12) at pH 8.48, 37 °C.

$$k_{obsd} = \left[k_{SH}^{w} + k_{SH}^{OH}a_{OH^-} + \frac{K_a^{SH}}{a_{H^+}}(k_S^{w} + k_S^{OH}a_{OH^-}) + K_N'(k_{SMe}^{w} + k_{SMe}^{OH}a_{OH^-}) \right] \Big/ \left[1 + \frac{K_a^{SH}}{a_{H^+}} + K_N' \right] \quad (14)$$

$$k_{obsd} = \left[k_{SH}^{w} + k_{SH}^{OH}a_{OH^-} + k_{SH}^{MOH}[Mg^{2+}]a_{OH^-} + \frac{K_a^{SH}}{a_{H^+}}(k_S^{w} + k_S^{OH}a_{OH^-}) + K_N'(k_{SMe}^{w} + k_{SMe}^{OH}a_{OH^-} + k_{SMe}^{MOH}[Mg^{2+}]a_{OH^-}) \right] \Big/ \left[1 + \frac{K_a^{SH}}{a_{H^+}}(1 + K_M[Mg^{2+}]) + K_N' \right] \quad (15)$$

of HPLC peak areas corresponding to $[SMe^{\pm}]$ and $[S]_{total}$ ($[S]_{total} = [SH^{\pm}] + [S^-]$ appears as a single peak on the HPLC), eq 16.

$$K_N = \frac{[SMe^{\pm}]}{[S]_{total}} \frac{K_a^{SH} + a_{H^+}}{a_{H^+}} \frac{[2\text{-MeIm}]}{[1,2\text{-diMeIm}]} \quad (16)$$

A value of $K_N = 0.079$ was obtained. Calculated K_N' values based on $K_N = 0.079$ are included in Table IV. They show that under most conditions $K_N' > 1$; i.e., $SMe^{\pm}$ was favored over $SH^{\pm}$. Figure 6 represents a plot of k_{obsd} vs K_N' in the absence of Mg^{2+} at pH 8.48. The values of k_{obsd} used in this plot were extrapolated to zero 1,2-diMeIm concentration, in order to correct for slight buffer catalysis, which was observed at high buffer concentrations. The initial slope of this plot is given by eq 17 ($k_{SMe}^{OH}a_{OH^-} \ll k_{SMe}^{w}$

$$\text{slope} = \frac{k_{SMe}^{w}}{1 + \frac{K_a^{SH}}{a_{H^+}}} \quad (17)$$

at pH 8.48, see below) from which we calculate $k_{SMe}^{w} = 1.33 \times 10^{-1}$ h^{-1}. Alternatively, one may plot $(k_{obsd} - \text{int})^{-1}$ vs $(K_N')^{-1}$ where int refers to k_{obsd} in the absence of 1,2-diMeIm ($K_N' = 0$). This inversion plot (not shown) is approximated by eq 18. It yields

$$\frac{1}{k_{obsd} - \text{int}} \approx \frac{1 + K_a^{SH}/a_{H^+}}{k_{SMe}^{w}K_N'} + \frac{1}{k_{SMe}^{w}} \quad (18)$$

$k_{SMe}^{w} = 1.30 \times 10^{-1}$ h^{-1} from its intercept and $1 + K_a^{SH}/a_{H^+} = 5.52$ from the ratio slope/intercept. The value 5.52 is close to the value of 6.5 calculated for $1 + K_a^{SH}/a_{H^+}$ on the basis of the known pK_a^{SH}. This close agreement is equivalent to a kinetic confirmation of K_N that was determined by HPLC analysis.

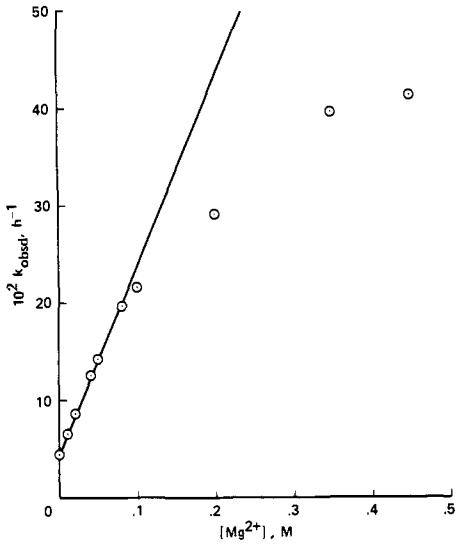

Figure 7. Hydrolysis of 2-MeImpG as a function of Mg^{2+} concentration, in the presence of 1,2-diMeIm and 2-MeIm, with $K_N' = 3.55$ (K_N' defined in eq 12) at pH 8.75, 37 °C.

Figure 7 shows a plot of k_{obsd} vs $[Mg^{2+}]$ at pH 8.75 and $K_N' = 3.55$. The initial slope of 1.82 M^{-1} h^{-1} is given by

$$\text{slope} = \frac{(k_{SH}^{MOH} + K_N' k_{SMe}^{MOH}) a_{OH^-}}{1 + \frac{K_a^{SH}}{a_{H^+}} + K_N'} \quad (19)$$

Solving for the only unknown affords $k_{SMe}^{MOH} = 6.14 \times 10^5$ M^{-1} h^{-1}.

The plot in Figure 7 displays a considerably stronger downward curvature than the plot in Figure 3 in the absence of 1,2-diMeIm. We attribute this enhanced curvature to the rate of the Mg^{2+}-catalyzed conversion of $SMe^{\pm}$ to products ($k_{SMe}^{MOH}[Mg^{2+}]a_{OH^-}$) becoming comparable to the rate of the $SMe^{\pm} \rightarrow SH^{\pm}$ step in Scheme V. In other words, $SH^{\pm} \rightleftarrows SMe^{\pm}$ is no longer a fast equilibrium and the reaction $SH^{\pm} \rightarrow SMe^{\pm}$ becomes co-rate-limiting with $SMe^{\pm} \rightarrow$ products. This interpretation is supported by HPLC data, which show a decrease in the $[SMe^{\pm}]/[SH^{\pm}]$ ratio at high $[Mg^{2+}]$.

In an attempt to measure k_{SMe}^{OH} for the reaction of $SMe^{\pm}$ with OH^-, we performed experiments in strongly basic solution and at high [1,2-diMeIm]/[2-MeIm] ratios (high K_N'). The difference in k_{obsd} obtained from experiments in the presence and absence of 1,2-diMeIm and 2-MeIm should be given by eq 20 ($K_a^{SH}/a_{H^+} \gg 1 + K_N'$). The results are summarized in Table V. One

$$\Delta = k_{obsd}(\text{eq 14}) - k_{obsd}(\text{eq 1}) = \frac{K_N'}{K_a^{SH}}(k_{SMe}^{w} a_{H^+} + K_w k_{SMe}^{OH}) \quad (20)$$

possible interpretation of the data in the table is that Δ is indeed given by eq 20 and that eq 20 simplifies to $\Delta = K_N' K_w k_{SMe}^{OH}/K_a^{SH}$ at $[NaOH] \geq 0.02$ M from which an approximate k_{SMe}^{OH} of 19.7 M^{-1} h^{-1} may be calculated. There are two problems with this interpretation: (1) The calculated k_{SMe}^{OH} value is much lower than k_{SH}^{OH} (100–170 M^{-1} h^{-1}, see below), which is difficult to understand since the reactivities of $SMe^{\pm}$ and $SH^{\pm}$ are expected to be similar. (2) More seriously, the k_{SMe}^{w} value of 7.2×10^{-1} h^{-1} calculated for the water reaction from eq 20 at $[NaOH] < 0.02$ M is more than 5-fold higher than the value (1.3×10^{-1} h^{-1}) determined from eq 17 and 18. These discrepancies can be attributed to a breakdown of the equilibrium assumption for the $SH^{\pm} \rightleftarrows SMe^{\pm}$ process at high [NaOH] because the hydrolysis of $SMe^{\pm}$ becomes faster than its reversion to $SH^{\pm}$, and hence eq 14 and with it eq 20 is no longer valid. If one assumes that at the lowest [NaOH] (0.005 M) eq 20 is still a reasonably good approximation, a lower limit for $k_{SMe}^{OH} \geq 120$ M^{-1} h^{-1} may be obtained by solving eq 20 for k_{SMe}^{OH} with $k_{SMe}^{w} = 1.3 \times 10^{-1}$ h^{-1}.

Table VI. Hydrolysis of ImpG in the Presence of *N*-MeIm and Im at 37 °C

pH	[*N*-MeIm],[a] M	[Im],[a] M	K_N'[b]	$[Mg^{2+}]$	k_{obsd}, h^{-1}
7.27	0.06		*c*	0	0.532
	0.12				0.803
	0.24				1.063
	0.36				1.27
	0.48				1.44
7.29	0.293	0.012	6.37	0	0.44
	0.468	0.019			0.46
7.31	0.287	0.023	3.25	0	0.252
	0.379	0.030			0.280
	0.46	0.037			0.320
	0.57	0.046			0.340
8.00	0.392	0.0043	23.7	0	0.49
				0.01	0.55
				0.02	0.54
				0.04	0.65
				0.05	0.65
				0.08	0.77
				0.10	0.86
				0.20	1.13
				0.40	1.59
				0.45	1.71
				0.50	1.77

[a] Concentrations refer to free base calculated from pH, total buffer concentration, and the pK_a's measured at room temperature, pK_a = 7.24 (Im), 7.44 (*N*-MeIm). [b] K_N' defined by eq 13; $K_N = 0.26 \pm 0.03$ determined by HPLC analysis at pH 7.29 and 7.31. Determination of K_N as described in the text. [c] K_N' varies because of increasing [*N*-MeIm]/[Im]; Im formed from hydrolysis of ImpG. [Im] ≤ 0.001 M during reaction.

Table VII. Hydrolysis of ImpG in the Presence of *N*-MeIm and Im in NaOH Solutions, without Mg^{2+} at 37 °C

	$10^2 k_{obsd}$, h^{-1}		
[NaOH]	$K_N' = 0$[a,b]	$K_N' = 65$[a,c]	Δ
0.01	0.380	0.909	0.529
0.02	0.73	0.912	0.182
0.04	1.28	1.235	≈0
0.05	1.69	1.51	≈0
0.08	2.77		
0.10	3.34		

[a] K_N' defined in eq 13; $K_N = 0.26$ determined by HPLC. [b] No *N*-MeIm/Im added; data from Table I. [c] [*N*-MeIm] = 0.5 M, [Im] = 0.002 M, [ImpG] = 5×10^{-4} M.

***N*-MeImpG.** Our study of this compound was more limited, but the results were similar to those obtained with 1,2-diMeImpG. K_N determined by HPLC analysis is 0.26 ± 0.03. The kinetic data are reported in Tables VI and VII. One set of data (pH 7.27, Table VI) was obtained as a function of increasing [*N*-MeIm] but without addition of Im. Under these conditions K_N' is not strictly constant throughout a kinetic run, which was reflected in less than perfect first-order kinetic plots. The k_{obsd} values are therefore only approximate. These experiments showed a strong dependence of k_{obsd} on [*N*-MeIm] (□, Figure 8) as one would expect since K_N' increases with [*N*-MeIm]. The curvature is probably due to saturation, i.e., nearly complete conversion of $SH^{\pm}$ to $SMe^{\pm}$ at high [*N*-MeIm] since in the absence of Im K_N' becomes very high. From an inversion plot (not shown) one obtains an approximate value of ~1.8 h^{-1} for the plateau, which, according to the above interpretation, should correspond to k_{SMe}^{w}.

The data at pH 7.29 and 7.31, which were obtained at constant K_N', support the above conclusion. After correction for the slight buffer catalysis (Figure 8) by extrapolation to zero buffer concentration, k_{obsd} is given by

$$k_{obsd} = \frac{k_{SH}^{w} + K_N' k_{SMe}^{w}}{1 + \frac{K_a^{SH}}{a_{H^+}} + K_N'} \quad (21)$$

from which we calculate an average $k_{SMe}^{w} = 1.76$ h^{-1}.

The dependence of k_{obsd} on $[Mg^{2+}]$ determined at pH 8.00 and

Table VIII. Summary of Rate and Equilibrium Constants for the Hydrolysis of ImpG, 2-MeImpG, 2-MeImpA, *N*-MeImpG, and 1,2-diMeImpG in Water in the Absence and Presence of Mg^{2+} (Ca^{2+}) at 37 °C

param	ImpG	*N*-MeImpG	2-MeImpG	1,2-diMeImpG	2-MeImpA
pK_a^{SH}	6.01 ± 0.20		7.74 ± 0.20		7.74[d]
K_M, M^{-1}	3.86 ± 1.1		0.93 ± 0.07		1.02 ± 0.1
K_N	0.26 ± 0.03		0.079 ± 0.005		
k_{SH}^{w}, h^{-1}	0.557 ± 0.02		$(3.32 \pm 0.2) \times 10^{-2}$		
k_{SMe}^{w}, h^{-1}		1.76 ± 0.2		0.13 ± 0.02	
k_S^{w}, h^{-1}	$(3.2 \pm 0.2) \times 10^{-4}$[a]		$[2.0 \times 10^{-4}]$[a]		
k_{SH}^{OH}, $M^{-1}\ h^{-1}$	$[1.49 \times 10^{4}]$[b]		$\approx 1.73 \times 10^{2}$[b]		
k_{SMe}^{OH}, $M^{-1}\ h^{-1}$		$\geq 3.6 \times 10^{3}$		$\geq 1.1 \times 10^{2}$	
k_S^{OH}, $M^{-1}\ h^{-1}$	0.33 ± 0.02		$(2.13 \pm 0.16) \times 10^{-2}$		
k_{SH}^{MOH}, $M^{-2}\ h^{-1}$	$(3.6 \pm 0.3) \times 10^{6}$ 7.3×10^{5}[c]		$(1.0 \pm 0.1) \times 10^{5}$ 1.8×10^{4}[c]		$(0.96 \pm 0.11) \times 10^{5}$
k_{SMe}^{MOH}, $M^{-2}\ h^{-1}$		7.91×10^{6}		6.14×10^{5}	

[a] Assuming $k_S^{w} \gg k_{SH}^{OH} K_w / K_a^{SH}$, see text. [b] Assuming $k_{SH}^{OH} K_w / K_a^{SH} \gg k_S^{w}$, see text; calculated with $K_w = 2.1 \times 10^{-14}\ M^{-2}$. [c] Value refers to Ca^{2+}. [d] Assumed to be the same as for 2-MeImpG.

Table IX. Structure–Reactivity Correlations

	rate constant ratio	$\beta_{lg} = (d \log k)/(d\ pK_{lg})$[a]
k_{SH}^{w}(ImpG)/k_{SH}^{w}(2-MeImpG)	16.8	−1.38
k_{SMe}^{w}(*N*-MeImpG)/k_{SMe}^{w}(1,2-diMeImpG)	13.5	−1.19
[k_S^{w}(ImpG)/k_S^{w}(2-MeImpG)]	[≈1.6][c]	[>−0.20][c]
[k_{SH}^{OH}(ImpG)/k_{SH}^{OH}(2-MeImpG)]	[≈86][d]	[−2.17][d]
k_{SMe}^{OH}(*N*-MeImpG)/k_{SMe}^{OH}(1,2-diMeImpG)	≈32.7	≈−1.59
k_S^{OH}(ImpG)/k_S^{OH}(2-MeImpG)	15.5	−1.34
k_{SH}^{MOH}(ImpG)/k_{SH}^{MOH}(2-MeImpG)	36.0 (40.6)[b]	−1.75 (−1.81)[b]
k_{SMe}^{MOH}(*N*-MeImpG)/k_{SMe}^{MOH}(1,2-diMeImpG)	12.9	−1.17

[a] pK_{lg} = 7.06 (Im), 7.95 (2-MeIm), 7.22 (*N*-MeIm), and 8.17 (1,2-diMeIm) at 37 °C. [b] Values in parentheses for Ca^{2+}. [c] See footnote *a* in Table VIII. [d] See footnote *b* in Table VIII.

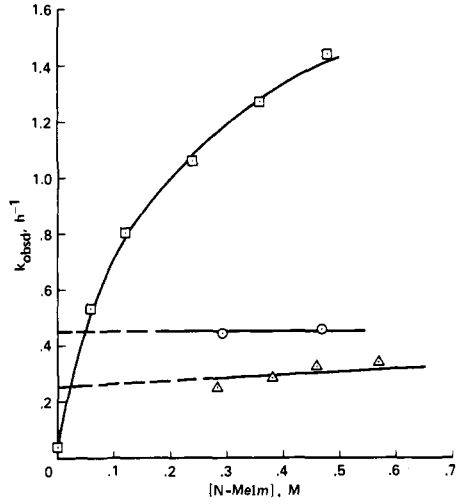

Figure 8. Hydrolysis of ImpG as a function of *N*-MeIm concentration in the presence of *N*-MeIm and Im at pH 7.27 in *N*-MeIm buffer only, squares; at pH 7.29 with $K_N' = 6.37$, circles; at pH 7.31 with $K_N' = 3.25$, triangles (K_N' defined in eq 13), at 37 °C.

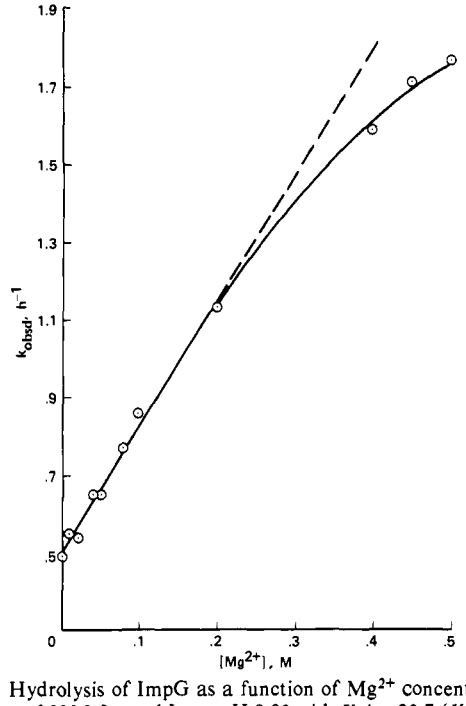

Figure 9. Hydrolysis of ImpG as a function of Mg^{2+} concentration in the presence of *N*-MeIm and Im at pH 8.00 with $K_N' = 23.7$ (K_N' defined in eq 13), at 37 °C.

$K_N' = 23.7$ (Figure 9) affords $k_{SMe}^{MOH} = 7.91 \times 10^{6}\ M^{-2}\ h^{-1}$ via eq 19. Our attempt to determine k_{SMe}^{OH} via eq 20 at high [NaOH] failed for the same reasons as with 2-MeImpG, i.e., because of the breakdown of eq 20. Applying eq 20 to the lowest [NaOH] and solving eq 20 for k_{SMe}^{OH} with $k_{SMe}^{w} = 1.76\ h^{-1}$ affords $k_{SMe}^{OH} \gtrsim 3.6 \times 10^{3}\ M^{-1}\ h^{-1}$.

Discussion

Mechanism of Hydrolysis of ImpG and 2-MeImpG in the Absence of Mg^{2+}. Table VIII summarizes all rate and equilibrium constants determined in this study. As described in the Results the kinetic data in the absence of Mg^{2+} are well accounted for by the mechanism of Scheme II. There remains an ambiguity, though, because the pH dependence of k_{obsd} does not allow a distinction between the reaction of S^- with water (k_S^{w}) and its kinetic equivalent, the reaction of $SH^{\pm}$ with OH^- (k_{SH}^{OH}). Note that even though the k_S^{w} pathway requires the expulsion of the leaving group as an amide ion, this is a viable reaction because the pK_a of imidazoles acting as acids (=14.5 for imidazole[11]) is much lower than the pK_a of aliphatic amines (≈35 for ethylamine[12]).

Some qualitative conclusions regarding the competition between the two pathways may be drawn by comparing the reactivities of ImpG and 2-MeImpG. If the k_{SH}^{OH} pathway was dominant for both substrates ($k_{obsd} = k_{SH}^{OH} K_w / K_a^{SH}$ for plateau at high pH), one would calculate a ratio k_{SH}^{OH}(ImpG)/k_{SH}^{OH}(2-MeImpG) of 86. Since the leaving group pK's differ by only 0.89

(11) Wolba, H.; Isensee, R. W. *J. Org. Chem.* **1961**, *26*, 2789.
(12) Streitweiser, A., Jr.; Heathcock, C. H. *Introduction to Organic Chemistry*, 3rd ed.; Macmillan: New York, 1985; p 1156.

(Table IX, footnote *a*), this would translate into a $\beta_{1g} \approx -2.17$. If, on the other hand, k_S^w was the prevailing pathway for both substrates ($k_{obsd} = k_S^w$), the ratio $k_S^w(\text{ImpG})/k_S^w(\text{2-MeImpG})$ of ≈ 1.6 would yield a $\beta_{1g} \approx -0.20$ (assuming that the pK_a difference between the imidazole anions is the same as for the imidazoles).

In comparison with the β_{1g} values calculated for several other processes (Table IX), −2.17 is appreciably more negative while −0.20 is dramatically less negative than the other β_{1g} values. A plausible explanation for these anomalous β_{1g} values (a more detailed discussion of the β_{1g} values in Table IX will be presented below) is that for ImpG the k_S^w pathway is more important than the k_{SH}^{OH} pathway while for 2-MeImpG the opposite is true. For example, if 85% of hydrolysis of ImpG went through k_S^w, 15% through k_{SH}^{OH}, while 15% of the reaction of 2-MeImpG went through k_S^w and 85% through k_{SH}^{OH}, one would obtain $\beta_{1g} = -1.08$ for the k_S^w pathway and −1.33 for the k_{SH}^{OH} pathway. Without taking the above numerical example too literally, we may conclude that for ImpG the k_S^w value given in Table VIII (3.2×10^{-4} h^{-1}) is an upper limit that is close to the true value, probably $3.2 \times 10^{-4} > k_S^w > 2.0 \times 10^{-4}$, while the true k_{SH}^{OH} value is substantially below the upper limit of 1.49×10^4 M^{-1} h^{-1} given in Table VIII. Conversely, for 2-MeImpG it is k_{SH}^{OH} that is close to the upper limit (1.73×10^2 M^{-1} h^{-1}), probably $1.73 \times 10^2 > k_{SH}^{OH} > 1.2 \times 10^2$, while k_S^w must be significantly below its upper limit of 2.0×10^{-4} h^{-1}. Two points regarding the above conclusions are noteworthy. (1) The estimate for k_{SH}^{OH} is very close to $k_{SMe}^{OH} \geq 1.1 \times 10^2$ M^{-1} h^{-1}, which is a reasonable result in view of the expected similar reactivities of $SH^{\pm}$ and $SMe^{\pm}$. (2) It seems reasonable that it is ImpG for which the k_S^w pathway is preferred over the k_{SH}^{OH} pathway since $pK_a^{SH} = 6.01$ is much lower than that for 2-MeImpG ($pK_a^{SH} = 7.74$); at the pH values where ImpG is predominantly in the $SH^{\pm}$ form, the hydroxide activity is apparently too small for the OH^- reaction to be very important.

It should be mentioned that in a previous study[7] of the hydrolysis of 2-MeImpG carried out in a lower pH range at 75 °C it was found that at pH < 3 k_{obsd} increases with decreasing pH. The mechanistic possibilities that may account for such acid catalysis have been discussed.[7]

Mechanism of Mg^{2+} Catalysis. The experiments with the N-methylated substrates show clearly that the Mg^{2+} catalysis must be accounted for by the reaction of $SH^{\pm}$ with OH^- (Scheme IV) rather than reaction of S^- with water (Scheme III). This may be unexpected in view of the above conclusion that in the *absence* of Mg^{2+} both pathways compete and also in view of the expectation of an electrostatically more favorable complexation between Mg^{2+} and S^- than with $SH^{\pm}$. With respect to the first point we note that our findings are consistent with the observation that OH^--catalyzed hydrolyses of amides[13] and esters[14] are much more strongly accelerated by metal ions than water-promoted hydrolyses; with respect to the second point one needs to be reminded that what determines reactivity is not so much complex stability between metal ion and the *reactant* but stabilization of the *transition state* by the metal ion (more on transition states below).

The mechanistic alternatives, which we shall discuss, all involve complexation of the magnesium ion at the reaction site since it would be difficult to explain the strong catalytic action of Mg^{2+} by an interaction of the metal ion with a part of the molecule remote from the reaction site, such as the guanine moiety. This point may be self-evident, but it is nevertheless rewarding that the Mg^{2+} effect on the hydrolysis of 2-MeImpA is virtually the same as that on the hydrolysis of 2-MeImpG, which is completely consistent with this assumption. The point becomes even more compelling when the ionization states of the guanine and adenine moieties are taken into consideration: the former is anionic at pH ≥ 9.2;[15] the latter is not.

One mechanistic possibility is that the reaction involves complexation between $SR^{\pm}$ (R = H or Me) and Mg^{2+} followed by nucleophilic attack by OH^-. This is shown in eq 22, with k_{SR}^{MOH} given by eq 23.

$$SR^{\pm} + Mg^{2+} \overset{K_{SR}^M}{\rightleftharpoons} SR^{\pm}\cdot Mg^{2+} \quad (22a)$$

$$SR^{\pm}\cdot Mg^{2+} + OH^- \xrightarrow{k_{OH}} \text{products} \quad (22b)$$

R = H or Me

$$k_{SR}^{MOH} = K_{SR}^M k_{OH} \quad (23)$$

The transition state would derive its stabilization from complexation of Mg^{2+} by the two phosphate oxygens (**1**).[16] For

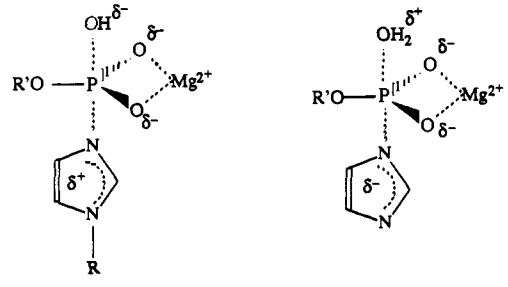

R = H or Me, R' = guanosine

1 **2**

comparison purposes, the likely transition state for the (undetected) Mg^{2+}-catalyzed reaction of S^- with water is shown as **2**.[16] Possible reasons why **1** is more favorable than **2** include the following. (1) In both transition states there is a repulsive interaction between Mg^{2+} and a partial positive charge. In **1** the positive charge is on the imidazole moiety, delocalized and farther removed, while in **2** it is on the attacking water, localized and closer to Mg^{2+}. (2) In both transition states there is a stabilizing interaction between Mg^{2+} and a partial negative charge. In **1** the partial negative charge is on the attacking OH^-, localized and close, while in **2** it is on the imidazole, delocalized and remote. Both factors tend to favor **1** over **2**.

An alternative mechanism is shown in eq 24; it involves reaction of the substrate with

$$Mg^{2+} + OH^- \overset{K_{MgOH}}{\rightleftharpoons} MgOH^+ \quad (24a)$$

$$SR^{\pm} + MgOH^+ \xrightarrow{k_{MgOH}} \text{products} \quad (24b)$$

$MgOH^+$, which is in equilibrium with Mg^{2+} and OH^-, and k_{SR}^{MOH} (R = H or Me) is given by

$$k_{SR}^{MOH} = K_{MgOH} k_{MgOH} \quad (25)$$

Simple attack by $MgOH^+$ on the substrate as shown in **3** would

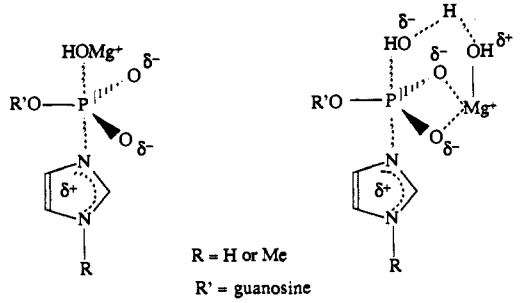

R = H or Me

R' = guanosine

3 **4**

not be able to explain the large catalytic effect by Mg^{2+}. A measure of this effect would be the k_{SH}^{MOH}/k_{SH}^{OH} and

(13) Fife, T. H.; Przystas, T. J. *J. Am. Chem. Soc.* **1986**, *108*, 4631.
(14) Fife, T. H.; Przystas, T. J. *J. Am. Chem. Soc.* **1985**, *107*, 1041.
(15) $pK_a = 9.2$, N_1–H of guanine: Ts'o, P. O. P., Ed. *Basic Principles in Nucleic Acid Chemistry*; Academic Press: New York, 1974; Vol. I, p 462.

(16) An alternative possibility is that Mg^{2+} is associated with only one of the phosphate oxygens.[17]

$k_{SMe}^{MOH}/k_{SMe}^{OH}$ ratios: they are $>2.4 \times 10^2$ for ImpG, $<2.2 \times 10^3$ for *N*-MeImpG, $\approx 5.8 \times 10^2$ for 2-MeImpG, and $<5.6 \times 10^3$ for 1,2-diMeImpG. Expressing k_{MgOH} as k_{SR}^{MOH}/K_{MgOH} (eq 25) with $K_{MgOH} \approx 150$[18] yields k_{MgOH}/k_{SR}^{OH} (R = Me or H, ratio of reactivity of $MgOH^+$ vs OH^-) > 1.6 for ImpG, <14.7 for *N*-MeImpG, ≈3.9 for 2-MeImpG, and ≤37.2 for 1,2-diMeImpG. In other words, the less basic $MgOH^+$ is more reactive than the more basic OH^- with all four substrates, which is unreasonable. A transition state, such as **4**,[16] which includes interaction of the phosphate oxygens with Mg^{2+}, could, however, account for the higher reactivity of $MgOH^+$ compared to that of OH^-. Similarly, enhanced reactivity of $MgOH^+$ in the hydrolysis of phosphorylated pyridines has recently been reported by Herschlag and Jencks[19] who describe the phenomenon as induced intramolecularly and attribute it to a transition state similar to **4**. On the basis of the available data, a distinction between **1** and **4** cannot be made.

Structure–Reactivity Relationships. A. Mg^{2+} Binding Constants. The equilibrium constants, K_M, for complexation of Mg^{2+} and ImpG or 2-MeImpG are approximately 4.0 and 1.0 M^{-1}, respectively (Table VIII). This compares with K_M values ranging between 4.6 and 14.8 M^{-1} for Mg^{2+} association with various phosphate dianions of the type **5** and **6**.[20] One would have

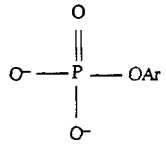

5

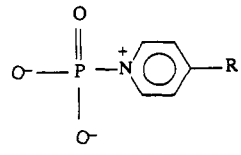

6

expected that ImpG and 2-MeImpG should be much worse complexing agents for Mg^{2+} because of the smaller negative charge and lower basicity.[17] Hence the rather small difference in the K_M values is surprising and suggests the presence of another factor in ImpG and 2-MeImpG that enhances complex stability. Molecular models indicate that there exists a conformation of ImpG and 2-MeImpG in which the OH group in the 3-position of the ribose ring can act as an additional binding site for the metal ion (**7**)[16] and presumably enhance K_M. This could also explain the

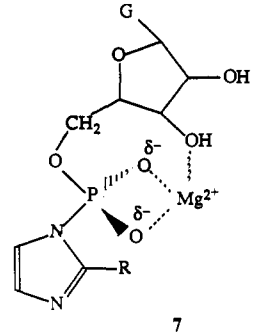

7

4-fold decrease in K_M that results from introducing a methyl group (R = Me) in the 2-position of the imidazole moiety: it sterically encumbers the Mg^{2+} binding site. Rotating the imidazole moiety by 180° would not help because of steric interference of the methyl group with the ribose oxygen in the 5-position. It should be mentioned, though, that the 3-OH group has been shown not to be involved in Mg^{2+} complexation by D-ribose 5′-monophosphate.[17] This result would argue against **7**, except that the lower basicity and smaller negative charge of ImpG and 2-MeImpG may render its complexes potentially more prone to extra stabilization by the 3-OH group than that of D-ribose 5′-monophosphate, which is a phosphate *di*anion.

It should be noted that the *transition state* of the Mg^{2+}-catalyzed reactions (**1** or **4**) cannot adopt the conformation shown in **7** because the ribose moiety would obstruct the trajectory of the attacking nucleophile.

B. Leaving Group Effects. In Table IX we have summarized rate constant ratios that measure the effect of changing the leaving group from imidazole to 2-methylimidazole, from *N*-methylimidazole to 1,2-dimethylimidazole, and from imidazole anion to 2-methylimidazole anion. The table also lists β_{lg} values derived from the ratios. In calculation β_{lg} for the comparison of imidazole anion with 2-methylimidazole anion, it was assumed that the pK_a difference of the two leaving groups is the same as that for imidazole vs 2-methylimidazole.

It should be emphasized that the β_{lg} values are subject to considerable experimental error, and hence we shall restrict our discussion to broad trends. The main reason for this large uncertainty is that β_{lg} was calculated on the basis of only two leaving groups, and pK_{lg} of these leaving groups differ by only 0.89 units (footnote *a* in Table IX). Thus an error in the rate constant ratios of say ±20%, which is a reasonable estimate for most ratios, translates into an uncertainty in β_{lg} of ±0.09.

With the exception of two entries, all β_{lg} values are seen to be in the range of about −1.2 to −1.8. The two values that fall significantly outside of this range are $\beta_{lg} = -2.17$ for k_{SH}^{OH}, calculated under the assumption that the k_{SH}^{OH} dominates over the k_S^w pathway for both substrates, and particularly $\beta_{lg} = -0.20$ for k_S^w, calculated under the assumption that the k_S^w pathway is dominant for both compounds. The reasons for these abnormal values have been discussed above.

The β_{lg} values in the order of −1.2 to −1.8 suggest that leaving group departure has made extensive progress at the transition state. This conclusion is difficult to reconcile with the rather strong Mg^{2+} catalysis, though. This catalysis requires a transition state with considerable buildup of negative charge on the phosphate oxygens, implying a substantial degree of nucleophile–P bond formation and little leaving group departure (associative transition state). Indeed, nucleophilic reactions on phosphoryl compounds of the same charge type as our substrates (one negatively charged phosphate oxygen, **8**) are known to have fairly associative transition

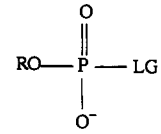

8

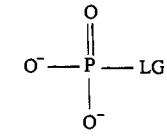

9

states;[20,21] this contrasts with phosphoryl compounds of the charge type **9**, which lead to dissociative transition states[20,21a,22-24] and whose reactions are at best very weakly catalyzed by Mg^{2+} or even inhibited by metal ions.[20] Incidentally, these changes from associative to dissociative transition states with charge type are also consistent with predictions based on reaction coordinate–energy contour diagrams.[19]

On the above basis, we conclude that there is a factor other than the pK_a of the leaving group that affects our β_{lg} values. This factor must be of steric origin and may be visualized as steric hindrance of solvation (or of Mg^{2+} complexation) at the phosphate oxygen by the 2-methyl group in the transition state. This effect is similar to the one invoked to explain the reduction in the K_M values brought about by the 2-methyl group; it reduces the rates of the 2-methylated substrates, thereby making β_{lg} more negative.

That the "true" β_{lg} values are probably much less negative than the values in Table IX may also be seen from the ratio k_{SH}^w/k_S^w for ImpG (1.74×10^3–2.78×10^3), which corresponds to $\beta_{lg} \approx$ −0.45 to −0.47. The fact that leaving groups of different charge

(17) (a) Massoud, S. S.; Sigel, H. *Inorg. Chem.* **1988**, *27*, 1447. (b) Sigel, H.; Massoud, S. S.; Tribolet, R. *J. Am. Chem. Soc.* **1988**, *110*, 6857.

(18) $pK_a \approx 11.5$ for $Mg^{2+} + H_2O \rightleftharpoons MgOH^+ + H^+$: Hogfeldt, E. Stability Constants of Metal Ion Complexes: Inorganic Ligands. *IUPAC Chemical Data Series 21*; Pergamon: New York, 1982; Part A.

(19) Herschlag, D.; Jencks, W. P., personal communication.

(20) Herschlag, D.; Jencks, W. P. *J. Am. Chem. Soc.* **1987**, *109*, 4665.

(21) (a) Kirby, A. J.; Varvoglis, A. G. *J. Chem. Soc. B* **1968**, 135. (b) Kirby, A. J.; Younas, M. *Ibid.* **1970**, 510, 1165. (c) Khan, S.; Kirby, A. J. *Ibid.* **1970**, 1172.

(22) Kirby, A. J.; Jencks, W. P. *J. Am. Chem. Soc.* **1965**, *87*, 3209.

(23) Bourne, N.; Williams, A. *J. Am. Chem. Soc.* **1984**, *106*, 7591.

(24) Numerous references cited in ref 20.

type are being compared may distort these β_{1g} values, but, due to the large pK_a difference between the leaving groups (7.28 pK units), these distortions would have to be very large to significantly change β_{1g}.[25]

Another comparison of interest is that between $SH^{\pm}$ and the corresponding $SMe^{\pm}$ forms. The relevant values are

$$k_{SMe}{}^{w}/k_{SH}{}^{w} = 3.16 \quad \text{for } N\text{-MeImpG vs ImpG}$$

$$k_{SMe}{}^{w}/k_{SH}{}^{w} = 3.91 \quad \text{for 1,2-diMeImpG vs 2-MeImpG}$$

$$k_{SMe}{}^{MOH}/k_{SH}{}^{MOH} = 2.20 \quad \text{for } N\text{-MeImpG vs ImpG}$$

$$k_{SMe}{}^{MOH}/k_{SH}{}^{MOH} = 6.14 \quad \text{for 1,2-diMeImpG vs 2-MeImpG}$$

The measured pK_{1g}'s of the N-methylated imidazoles are approximately 0.2 units higher than the pK_{1g}'s of the corresponding non-N methylated ones (footnote *a* in Table IX). However, since pK_{1g} for these latter reflect a statistical advantage of 0.3 units over the former, the statistically corrected pK_{1g} values should be used in comparing leaving group ability of the N-methylated with the non-N-methylated imidazoles. These corrected pK_{1g} values imply that the N-methylated imidazoles are slightly less basic and thus better leaving groups than the nonmethylated ones. The fact that the above listed rate constant ratios are all >1 is consistent with this conclusion, but the magnitude of these ratios seems too high for the small differences in leaving group basicities. These exalted ratios may be attributed to a reduced reactivity of the $SH^{\pm}$ type substrates due to hydrogen bonding of the NH^{+} proton to the solvent.

Implications for the Mechanism of Template-Directed Oligomerization. Even though unproven, it is likely that the mechanism of Mg^{2+}-catalyzed template-directed oligomerization of 2-MeImpG is similar to the one of the hydrolysis reaction. Thus, the monomer (2-MeImpG) presumably reacts in its $SH^{\pm}$ form and nucleophilic attack on 2-MeImpG by the oligomer occurs either with the ionized 3-OH group of the ribose moiety in a transition state similar to **1** or by $MgOH^{+}$-assisted attack of the unionized 3-OH group as in **4**.[26]

The empirically determined optimal conditions for template-directed oligomerization of 2-MeImpG are pH 8.0 and 0.2 M Mg^{2+}. We are unaware of a systematic study that has established that these conditions are truly the very best, but they are probably a good approximation to the true optimum. Such an optimum depends on a delicate balance of several factors, including the following.

(a) The pH should be high enough to favor the ionization of the 3-OH group of the ribose or to generate a high concentration of $MgOH^{+}$.

(b) Complexation of the growing oligoguanylate with the template [poly(C)], which depends on hydrogen bonding between G and C and which is a requirement for the reaction, is disfavored by the deprotonation of guanine at pH approaching or surpassing the pK_a of guanine (9.2).[15]

(c) The Mg^{2+} concentration should be high for efficient catalysis but not too high, in order to prevent formation of an unproductive complex ($S{\cdot}M^{+}$ in Scheme IV).

(d) The best conditions require not only an optimization of the oligomerization reaction but also a low rate for the competing hydrolysis.

It is clear from the above that only a systematic kinetic study of the oligomerization reaction could lead to the establishment of the true optimum conditions.

Conclusions

(1) The hydrolysis of ImpG and 2-MeImpG in the absence of metal ions occurs as shown in Scheme II. At pH < ~9 for ImpG (pH < ~10 for 2-MeImpG) the reaction of $SH^{\pm}$ with water ($k_{SH}{}^{w}$) is the dominant pathway, while at pH > 10.5 for ImpG (pH > 11.5 for 2-MeImpG) the reaction of S^{-} with OH^{-} ($k_{S}{}^{OH}$) is dominant. At the pH minima in Figure 1 there is a competition between the reaction of S^{-} with water ($k_{S}{}^{w}$) and of $SH^{\pm}$ with OH^{-} ($k_{SH}{}^{OH}$): for ImpG the $k_{S}{}^{w}$ pathway dominates over the $k_{SH}{}^{OH}$ pathway, while the opposite holds true for 2-MeImpG.

(2) In the presence of Mg^{2+} (or Ca^{2+}) the reaction of $SH^{\pm}$ with OH^{-} is dominant over the reaction of S^{-} with water (Scheme IV) for both substrates, a conclusion based on a comparison with the reactions of *N*-MeImpG and 1,2-diMeImpG. Our results are consistent with data on the hydrolysis of amides and esters, which show that metal ions catalyze hydroxide ion reactions much more strongly than water reactions.

(3) The most plausible transition state structures for Mg^{2+} catalysis are **1**[16] or **4**.[16] For the catalysis to be as effective as observed, bond formation must be quite advanced and leaving group departure should not have made much progress (associative transition state). The β_{1g} values of $\approx$–0.45 to –0.47 based on the ratio $k_{SH}{}^{w}/k_{S}{}^{w}$ for ImpG are consistent with relatively little progress in leaving group departure, but β_{1g} values calculated from rate constant ratios in Table IX are not. The latter indicate the presence of a rate-retarding steric effect by the 2-methyl group in 2-MeImpG and 1,2-diMeImpG.

(4) The association equilibrium constants between Mg^{2+} and ImpG or 2-MeImpG are unexpectedly high in comparison to similar constants for Mg^{2+} association with **5** and **6**. This suggests that the 3-OH group of the ribose moiety acts as an additional binding site (**7**).[16]

Acknowledgment. This research was supported by Grant No. NCC 2-534 from the Exobiology Program of the National Aeronautics and Space Administration. We thank Dr. S. Chang from the Planetary Biology Branch of the NASA/Ames Research Center for providing facilities and for discussion.

Supplementary Material Available: Tables S1–S3 of kinetic data on the hydrolysis of 2-MeImpG, ImpG, and 2-MeImpA in the presence of Mg^{2+} and Ca^{2+} (3 pages). Ordering information is given on any current masthead page.

(25) For example, if $k_{SH}{}^{w}/k_{S}{}^{w}$ were 10-fold larger, this would increase $|\beta_{1g}|$ by only 0.15 units.

(26) A reviewer has expressed skepticism regarding our tentative conclusion that the mechanism of Mg^{2+}-catalyzed oligomerization of 2-MeImpG may be similar to the one of the hydrolysis reaction, on the grounds that "the template provides a high concentration of both Mg^{2+} and phosphate ions near the substrate which will affect the mechanism in a manner different from the results observed in the absence of template." The fact that Mg^{2+} has been shown to undergo nonspecific binding with poly(C)[27] and that poly(C) has very little effect on the rate of hydrolysis of 2-MeImpG[28] would appear to argue against the reviewer's concerns.

(27) Diebler, H.; Secco, F.; Venturini, M. *Biophys. Chem.* **1987**, *26*, 193.

(28) Kanavarioti, A.; Chang, S., to be published.